ORIGINAL PAPER

A Laboratory Study of Shear Behaviour of Rockbolts Under Dynamic Loading Based on the Drop Test Using a Double Shear System

L. Li[1] · P. C. Hagan[1] · S. Saydam[1] · B. Hebblewhite[1] · C. Zhang[1]

Abstract

Rockbolts are widely used as an underground support element to resist the convergence and maintain the stability of excavations. However, shear failure of rockbolts is increasingly observed in jointed rock mass of underground tunnels, especially after being subjected to seismic events. At present, understanding of the mechanical response of rockbolts subjected to seismic or dynamic loading in shear is still unclear. To investigate the shear performance of rockbolts under dynamic loading condition, a series of tests were conducted using a drop mass of up to 185 kg from a maximum height of 3 m based on a double shear test (DST) system. Three variables were examined in the laboratory test including rockbolt diameter (8 mm and 16 mm), installation angle (90° and 45°) and input energy (drop height). The duration of the impact was 10–12 ms from release of the drop mass to first contact. By evaluating the DST system's displacement/velocity/acceleration–time characteristic and the amount of energy absorption, the shear performance of rockbolt was assessed. When sufficient energy is applied into the DST system, the deformation of the rockbolt is dominated by localized shear force. The transient force can rupture the rockbolt with little bending and without any obvious tensile elongation. It was found that the averaged dynamic shear load is less than the peak static shear load whether horizontally installed or installed at an angle. In conclusion, the effectiveness of rockbolts in resisting shear stress can differ significantly under static loading and dynamic loading condition; the difference is reflected in the level of shear deformation and amount of energy absorption. The shear capacity of a rockbolt under $1\ \text{s}^{-1}$ strain rate can be determined by the energy absorbed and average dynamic load. This approach can be applied to the support system design in rockburst-prone condition.

Keywords Dynamic loading · Strain rate · Double shear test · Rockbolt · Shear resistance

Abbreviations

M_1	A drop weight mass
M_2	The mass of middle block including the rockbolt
v_1	Initial velocity
v_2	The downward move velocity of the two rigid solids (weight and reinforced block)
F_a	The average dynamic force
Δv	Velocity change
$(M_1 + M_2)g$	The downward force includes the weight of the tup and middle block
$F_d(t)$	External dynamic force
$F_b(t)$	Upward force includes bolt resistant force
μN	Frictional force on the block surface
$p(t)$	Time-dependent force
$f_s(t)$	The combination of the system spring force
$f_D(t)$	Viscous damping force
$f_I(t)$	Inertial force
p	Contact force
k	Contact stiffness
R	The radii of the curvature of the body
E	Young's modulus and
v	Poisson's ratios
f_y	The static yield stress of the bar (MPa)
DIF	Dynamic increase factor
$\dot{\varepsilon}$	Strain rates
ε_p	True strain
$\dot{\varepsilon}_0$	Reference value of the strain rate
T	Temperature
T_{room}	Room temperature
T_{melt}	Melting temperature

✉ L. Li
   skylily616@gmail.com

1 School of Mining Engineering, UNSW Australia, Sydney, Australia

1 Introduction

Dynamic loading of rock support systems arising from rockbursts can result in high-stress loading in rockbolts leading to yielding of steel tendons, loosening of the rockbolt anchor, and in some cases causing complete failure of the rockbolt (Tannant et al. 1995).

The objective of a dynamic support system is to absorb the kinetic energy. Rock is prone to fail when the ground stress is higher than its strength. In this condition, loading of the support system is not solely a function of deadweight, but becomes a displacement controlled process (Li 2011). In high-stress rock conditions, rock support should be strong and also ductile, and should be capable of absorbing a large amount of deformation energy prior to failure (Li 2011). Figure 1 shows deformed rockbolt following a seismic event within a rockmass.

There has been limited study on the shear failure of rockbolt under dynamic loading, though the tensile behaviour has been assessed both in laboratory and in situ environment. However, a comprehensive underground support design requires knowledge of the capacity of rockbolts both in shear and tension.

The response of rockbolts is sensitive to the rate of loading. Hence, a thorough knowledge of material constitutive relationships and failure criteria is required to properly design an optimum support system at different loading rates. The drop test is commonly used to simulate the rockburst or blasting effect on the rock and rock support systems, which can give rise to a strain rate in order of 10 s^{-1} equivalent to a 250 μs loading duration (Bischoff and Perry 1991). A static loading rate of 10^{-5} s^{-1} is frequently used in standard uniaxial/triaxial compressive strength tests, which is equivalent to a 200 s loading duration to failure (Bischoff and Perry 1991). If higher stain rates are used then there is likely to be an increase in strength, for example, at strain rate of $1 \times 10^{-3} \text{ s}^{-1}$, there is likely to be a 20% increase in compressive strength.

Peak particle velocity is measured in underground excavations as an indication of the damage level of dynamic failures. However, Stacey (2011) stated that back analysis of ejection velocity from rockburst damage indicates inexplicably large magnifications of the peak particle velocities obtained from seismic measurements. This indicates there is still a lack of understanding of the mechanisms of action and interaction of support element in a rockburst environment (Stacey 2011). Therefore, design of support systems under dynamic loading is reliable only when the demand imposed on the support and the capacity of support systems under dynamic loading can be defined.

Ground motion induced by earthquakes, rockburst and blasting can differ significantly in magnitude and intensity. The strongest rockbursts often reach magnitude $M_L = 4$ (local magnitude) and sometimes may even exceed $M_L = 5$ (Zembaty 2011), which are of primary interest in this paper. Typical damage to the underground tunnel includes roof falling, floor heaving, working face eruption, and failure of support systems. Rock support is controllable in capacity design, installation pattern and different combinations. Therefore, it entails the importance of research in the capacity of rockbolt in resisting shear deformation under dynamic loading.

Stress measurement limitations at high strain rates have attracted researcher's attention because the inertial effect increases the measured load at the top of the specimen. This effect can be minimized by placing the load cell at the bottom unloaded end, as shown in Fig. 2. Top load cell includes an inertial force and a time lag exists between the top and

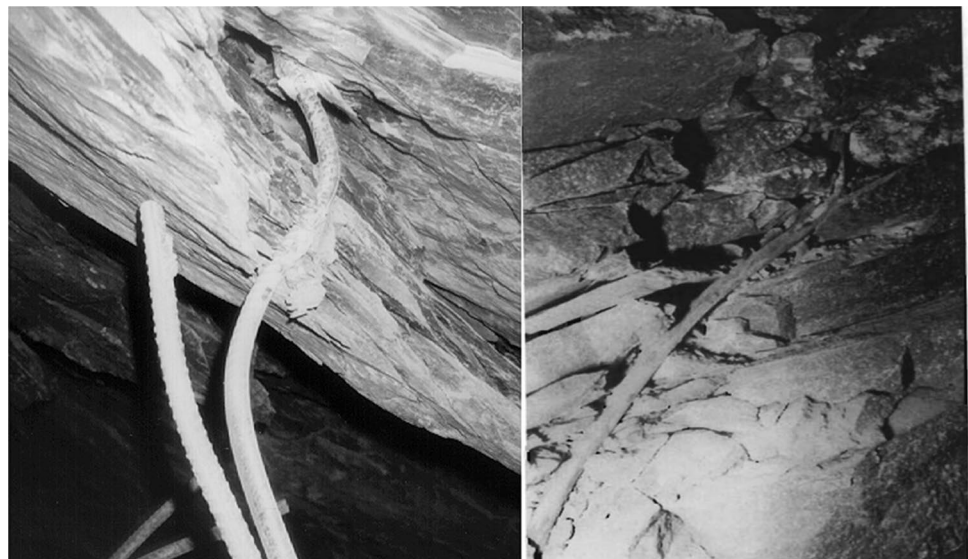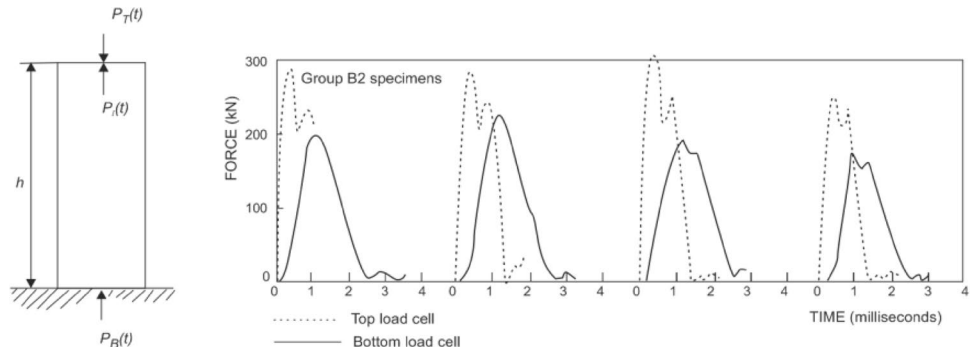**Fig. 1** Deformed rockbolts following a seismic event (Haile 1999b)

Fig. 2 Load measurement at the top and bottom of specimen loaded at strain rates between 0.1 and 1 s^{-1} (Chung 1978)

bottom load-cell signals caused by the initial propagation of the stress wave (Chung 1978). An explanation of how inertial effect works in high-speed load is given in Fig. 2 using P_I(t) to represent the inertial resistance along the length of the specimen. This issue should be paid attention and avoided during the dynamic load testing.

A previous double shear test under dynamic loading condition was conducted by Haile (1999a). A dynamic loading rate of 3 m s^{-1} was applied in a Terratek press; however, the test machine was initially settled under slow loading rate of 15 mm min^{-1}. In theory, the maximum shear strength of a steel bar is 50% of the ultimate tensile strength of the material according to the failure criterion as defined using Mohr's circle (Haile 1999a). However, laboratory testing results indicate a significant difference for a support system comprising rockbolt, grout and rock block (Aziz et al. 2003; Grasselli 2005; Haile 1999a; Li et al. 2014) with the calculation of Haile. For example, the static shear load and dynamic shear load are 140 kN and 124 kN, respectively, for a 16 mm rebar (Haile 1999a) with a tensile load of 156 kN. It should be noted that failure load is not a reliable parameter when considering impact loading. The impact force has a tremendous change when the drop mass penetrates into the target object with varied distance. Therefore, energy absorption would be suggested to be adopted in assessing the capacity of rockbolt under dynamic loading.

In this laboratory study, the shear displacement of a rockbolt and the velocity of acceleration of the sample were monitored. A series of drop tests were conducted by dropping a mass of up to 185 kg with a maximum height of 3 m on double shear test (DST) system. In addition, this designed drop tests could be used as the evaluation of rockbolt dynamic behaviour under high-strain-rate condition, such as rockburst condition. Three variables were examined in the laboratory test including rockbolt diameter (8 mm and 16 mm), installation angle (90° and 45°) and input energy (potential energy due to varying drop height). By evaluating the DST system's displacement/velocity/acceleration–time characteristic and the amount of energy absorption, the shear performance of rockbolt can be assessed. Moreover, the shear resistance of rockbolt was compared under quasi-static

loading and dynamic loading conditions, based on the results of a static double shear test (Li et al. 2016).

2 Double Shear Test Setup

2.1 Sample Preparation

Testing blocks were made from a cementitious mixture, cast in plywood moulds with dimensions of 300 mm × 300 mm × 200 mm, as shown in Fig. 3, to keep the strength consistency of every block used in double shear tests. Plastic conduits having diameters of 16 mm and 24 mm were placed in the moulds to create holes for later installation, respectively, 8 mm and 16 mm rockbolts after the cement mixture was poured into the moulds, the conduits were removed. The cylinder test sample had a measured UCS of 53 MPa.

After removed from the mould, each set of three blocks was joined together. A rockbolt was then inserted into the formed hole and grouted in place with a 60 MPa high-strength grout. Figure 4 shows the photographs of two types of rockbolts. They were used to study the load transfer mechanism by Aziz (2002–2015) and Jalalifar (2006). Table 1 lists the rib profile specifications of two types of rockbolts and the relevant parameters. Rockbolt tension tests

Fig. 3 The plywood moulds used for the sample casting

16 mm

8 mm

Fig. 4 The photographs of two types of rockbolts

Table 1 Specifications of rockbolts

Diameter (mm)	Mass per meter (kg)	Density (kg/m^3)	Rib spacing (mm)	Rib height (mm)
16	1.618	7850	11	1
8	0.406	7850	6	0.8

were carried out to measure the yield tensile strength, ultimate tensile strength, and Young's modulus, which are in accordance with the Australia Standards for tensile tests No AS 1391. The average values of yield tensile strength and ultimate tensile strength are shown in Table 2.

The steel in the rockbolt has an elastic modulus of 200 GPa and a density of 7850 kg/m^3. Figure 5a, b shows the cut-away view of the double shear test setup, with installation of the rockbolt and grout at 90° and 45°, respectively. Figure 5c shows the testing sample with steel casing confinement. Two steel plates are used for side confinement connected by four 24-mm bolts to constraint against any lateral movement.

2.2 Drop Test Rig and Instrumentations

The energy input was a function of the drop height and drop mass. The maximum theoretical energy available and the maximum impact velocity that each drop could reach not accounting for any frictions losses were 5439 J (185 kg×9.8 m s^{-2}×3 m) and 7.67 m s^{-1}, respectively. During a test, the drop tup is raised to a prescribed height above

the specimen using a hoist and chain system. After the tup reaches the desired test height it is released and falls down between the steel guide rails. Figure 6 shows the drop test rig and the position of high-speed camera. Figure 7 shows the prepared sample for impact testing. A 70-mm vertical space was reserved for the movement of the middle concrete block.

During the impact loading test, a displacement encoder and accelerometer were used to record the displacement and acceleration time histories of the DST system. The accelerometer was an integrated electronic piezoelectric (IEPE) type unit (Dytran model 3225F) with a sensitivity of 10.28 mV g^{-1}. The displacement measuring system consists of a Hewlett Packard HEDS-9200 encoder module reading a linear encoder strip with a pitch of 0.2 mm and a resolution of 0.05 mm. This produces a quadrature signal which is processed by an encoder interface unit. It outputs an analog voltage signal (-5 V to $+5$V) which is recorded by the data acquisition system. A high-speed camera was set at 2000 frames s^{-1} with an exposure time of 1/2000 s. A National Instruments logger was designed for data logging with a data acquisition frequency of 100 kHz.

During the drop test, it was found that the tup was rebounded off the test sample after first time contact within a very short period. As a result, only the first drop measurement is analysed for both displacement and acceleration.

2.3 Experimental Test Scheme

Table 3 details the test setups in this study by conducting a range of parametric analyses. Two major sets of drop testing were conducted to evaluate the influence of rockbolt installation angle, dropping height and rockbolt diameter.

In all tests, the displacement encoder and accelerometer were calibrated to improve the testing confinement (steel casing), which is the priority to be considered in case of concrete damaged by the impact load before the rockbolt bearing dynamic load. Drop height was adjusted according to the DST system damage magnitudes to determine the critical energy of shear failure.

The advantages of double shear tests under impact loading include the following: (1) impact load is characterized with single direction comparing the blasts and mining-induced seismicity, which is easy to study the shear behaviour of the rockbolt; (2) acceleration is generated by the free

Table 2 The mechanical properties of rockbolts

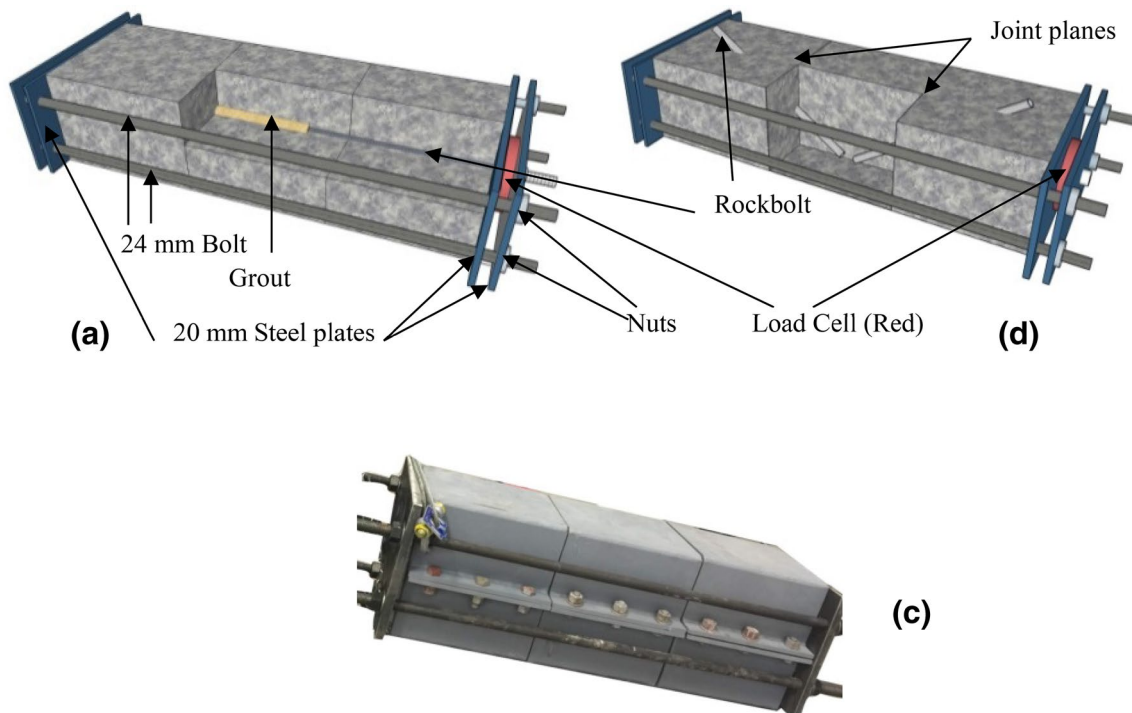| Rockbolt (mm)	Tensile yield stress (MPa)	Ultimate tensile stress (MPa)	Yield tensile load (kN)	Maximum tensile load (kN)	Young's modulus (GPa)	Average elongation (mm)	Percentage elongation (%)
16	570	662	118	134	200	90	9
8	449	570	25	29	200	50	5

Fig. 5 Schematic arrangement of double shear test with cut-away view. **a** Rockbolt at 90° to joints, **b** rockbolt at 45° and **c** test sample with steel casing confinement
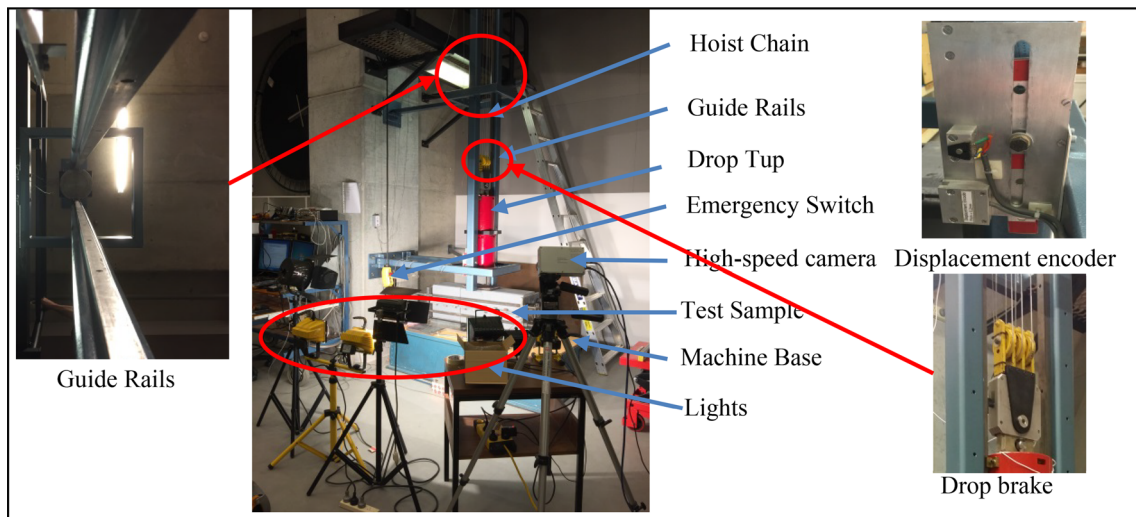

Fig. 6 The impact facility for double shear tests with high-speed camera setup and close-up view of displacement encoder, guide rails and drop brake

drop of weight on both concrete and rockbolt to investigate the interaction of rock and rockbolt; (3) double shear tests can avoid the rotation of the testing blocks during the impact loading comparing with the single shear tests; (4) double shear tests can effectively create the combination load of tensile and shear in rockbolt even when the grout is broken and the bond strength is lost.

3 Experimental Results

3.1 The Mechanical Response of Rockbolt Reinforced Joints

When a drop weight (mass M_1) impacts on the middle
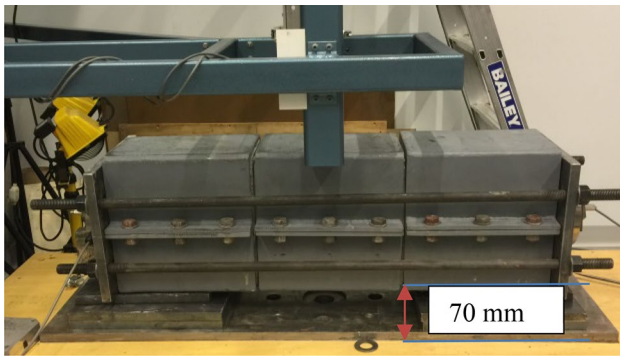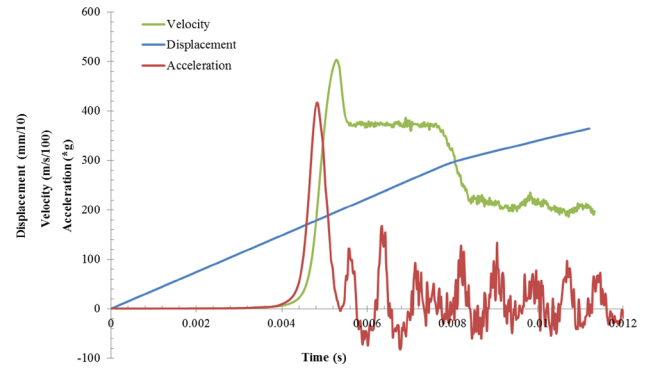
Fig. 7 The prepared sample for impact testing

Fig. 8 8-mm rockbolt with 45° inclined installation (I-1)

Table 3 Configuration of the dynamic tests

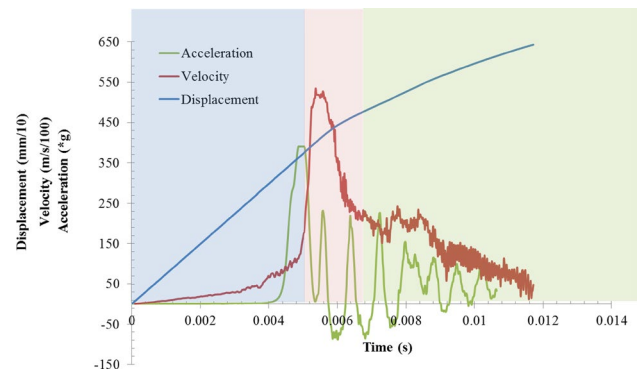| DST setup	Test number	Diameter (mm)	Drop height (m)	Max input energy (J)
90-Horizontal rebar	H-1	8	2.84	5149
	H-2	8	2	3626
	H-3	8	1.5	2719
	H-4	16	2.84	5159
45-Inclined rebar	I-1	8	1.5	2719
	I-2	8	1.5	2719
	I-3	8	1.2	1887
	I-4	16	2.85	5167

Fig. 9 16-mm rockbolt with 45° inclined installation (I-4)

block containing the rockbolt (mass M_2) at an initial velocity (v_1), the two rigid solids (weight and reinforced block) move downwards together at a new velocity (v_2). A drop weight of 185 kg travelling over a height of 2.8 m expected to result in an impact speed of 7.4 m s^{-1}. To avoid a jarring load transfer when the steel tup hits the steel casing, a carpet buffer was placed on the top of sample to prolong the duration of impact loading to reduce the strain rates.

The testing results show that the impact velocity of tup is around 5.03 m s^{-1}. The duration of impact through the carpet lasts around 3–3.5 ms. It should be noted that the recorded displacement also includes the thickness of carpet which is 18 mm. The initial velocity of the middle block immediately after the impact loading is obtained by employing the law of momentum conservation, as follows:

$$v_2 = v_1 M_1 / (M_1 + M_2), \quad (1)$$

where $M_2 = 60$ kg represents the mass of the middle block.

Therefore, the initial downward velocity of two solids is 3.8 m s^{-1}. The carpet plays a crucial role in overcoming the issue of inertial force. When the tup first strikes the specimen, a significant force is generated, because the

mass of the specimen has to be accelerated to the speed of the tup (Kong et al. 2013).

Single impact load is imparted on each specimen. The oscillations, mostly detectable on the contact surface of impact load, may result from the natural frequency of the steel material. Afterwards, the whole sample may rebound when the bolt resistance exceeds the impact force after the first impact touch, resulting in the acceleration change upwards. The middle block was suddenly stopped within 7 ms. Plastic deformation occurs once the transient dynamic load exceeded the elastic limit of the steel material.

Figures 8 and 9 illustrate displacement, velocity and acceleration processed filtered signals from a DST sample with inclined 8-mm and 16-mm rockbolts installed, respectively. Displacement gradually increased with the rate of increase decreasing with the time. Even though the displacement encoder was mounted on the tup, it could be inferred that the specimen has the same displacement as the tup because two solids move downwards together. The velocity curve is back calculated by the measured displacement and acceleration data. The maximum impact velocity is about 5.4 m s^{-1} in Fig. 8. An oscillating acceleration pattern was also observed,

particularly where the velocity is greatest (Haile 1999a) in Fig. 10.

Very large acceleration occurred during the impact loading representing a large transient dynamic load. It was recorded that the acceleration varied between 200 and 400 g (g is gravitational acceleration). This variation in acceleration corresponds to the rockbolt resistance in terms of different angles and diameters, and various drop heights. The free drop test is a more reliable simulation of a rockburst event than tests from a velocity-controlled machine. It can be observed from the research of Haile (1999a) that the velocity increases and decreases are symmetrical (Fig. 10). The loading from seismicity and rockburst occurs suddenly and has a short duration, similar to the situation of free weight drop.

In the following analysis, it is assumed that the impact process is an inelastic collision, and energy was dissipated through the sound, heat and friction between the interfaces of concrete, and the rest is absorbed energy within rockbolt. Meanwhile, the weight was assumed to behave as a rigid body and hence one can simply apply Newton's laws of motion. Because it allows quantitative calculations of dynamics, velocity changes can be determined when forces are applied. Based on this assumption, the motion can be expressed by
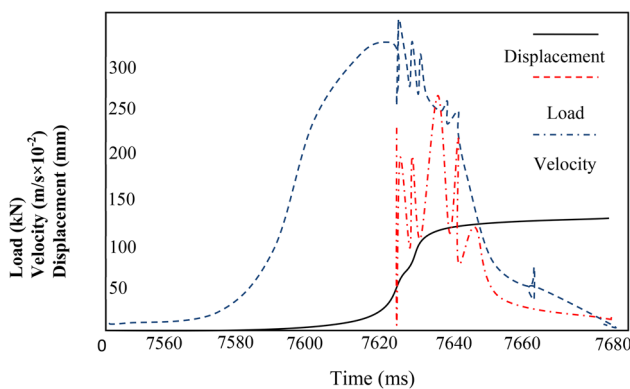
$$\int F_a dt = (M_1 + M_2)\Delta v, \tag{2}$$

Fig. 10 The load/velocity/displacement versus time curve from research of Haile (1999a)

where F_a is the average dynamic force. Assuming that the drop weight and concrete stopped moving, the average dynamic force 77.5 kN was applied to rockbolt. Where time is equal to 11.5 ms, total mass is 245 kg, and the change of velocity is 3.8 m s^{-1}. The ultimate tensile load is 29 kN for the 8-mm rockbolt. The measured dynamic shear load is 1.34 times of static ultimate tensile load. However, the instantaneous peak dynamic force will be higher than this calculated data. This will be further investigated by numerical modelling as the drop facility is incapable of measuring the dynamic shear capacity of the rockbolt.

The dynamic load provides an initial peak that generally exceeds the static capacity of the steel, followed by a trough and reloading to a peak or plateau that is referred to as the 'average' load or ultimate holding capacity of the bolt. The tendency of the dynamic load curve is similar to the acceleration curve.

The resulting curves can be divided into three stages of the impacting process. At first, the tup contacted the carpet and compressed the carpet until the specimen started bearing the load. Within this stage, the velocity of tup decreased rapidly, while the velocity of specimen increases dramatically, and then, the tup and specimen move downwards together. The rockbolt retards any movement of the block and undergoes a dramatic stress change. The rockbolt can be ruptured directly when the stress induced in the rockbolt exceeds the limit of dynamic strength of steel material. The last stage is when the two objects separate due to the bolt resistance force being larger than the dynamic force, stopping the movement of the specimen and the tup rebound upwards.

According to mechanical equilibrium conditions, force is mobilized in the DST system when the two objects move downward, as simplified in Fig. 11. The downward force includes the weight $[(M_1+M_2)g]$ of the tup and middle block and the external dynamic force $[F_d(t)]$; the upward force includes bolt resistant force $[F_b(t)]$ and frictional force on the block surface (μN). The dynamic force and the bolt resistant force are the variables with the time. The sum of downward loading equals the upward loading, as the below equation:

$$(M_1 + M_2)g + F_d(t) = 2F_b(t) + 2\mu N. \tag{3}$$

Fig. 11 The mechanical force during the impact loading
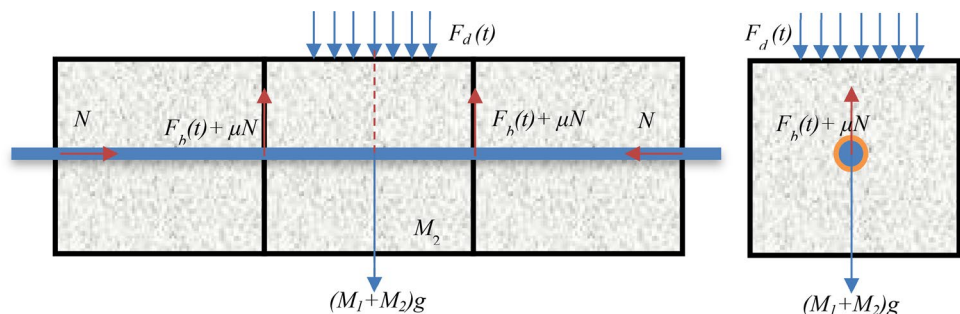
According to the research conducted by Hadjigeorgiou and Potvin (2011), the kinetic energy of the tup was significantly greater than that provided by gravity. The mass of weight also can be ignored to simplify the calculation.

It should be noted that this laboratory test is a first step towards understanding rockbolt shear performance under impact loading. This analysis focuses on the interaction of rockbolt and concrete block subjected to lateral dynamic load, simulating the shear moving of reinforced rock in seismicity event. Pure shear strength of a steel bar is approximately 50–60% of the tensile strength from static loading conditions. However, the mechanical response of rockbolt under dynamic shear load is different to the low strain rate. Substantial rapid plastic deformation was generated vertically in the rockbolt in 10–12 ms, as shown in Fig. 12, where the $N_d(t)$ is the mobilized tensile force along the rebar.

3.2 The Deformation of Rockbolt After Impact Loading

The modes of failure of the rockbolt are either shear or bending resulting from dynamic vertical shear and lateral tension. A unique situation occurred due to an imbalanced force subjected to sample, with one side of the rockbolt shearing off and the other side bending. Peak dynamic load, maximum acceleration and energy absorbed by the DST system are shown in Table 4. Of note is that apart from the work done
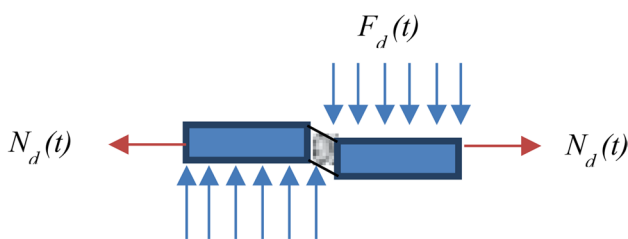

Fig. 12 The fracture-prone interface in the rockbolt

on the rock bolt shearing, a portion of the energy within the DST system is released in the form of heating and seismicity, which is out of the scope of this paper.

Impact tests started using the smaller diameter rockbolt with the maximum energy input. The rockbolt was cut into three sections after 12 ms. Input energy was adjusted by the drop height to determine the critical energy input and shear capacity. The height was adjusted from 2.84–2 to 1.5 m. The 8-mm horizontal rockbolt was ruptured on one side and bent on the other side resulting from a 1.5 m height drop. It can be speculated that the energy absorption (1274–1533 J) is close to the shear capacity of the rockbolt. For the inclined 8-mm rockbolt, the critical energy absorption is between 1801 and 2301 J. The inclined rockbolt installation required more energy for deformation compared to the horizontal rockbolt due to the larger vertical cross-sectional area and the tension resistance involved in the inclined scenario.

Figure 13 shows the failed reinforced DST system after impact loading. The strain rate of the rockbolt (longitudinally) is up to 1.5 s^{-1} for the 16-mm horizontal rockbolt (H-4) and 1.1 s^{-1} for the 8-mm horizontal rockbolt (H-3). The strain rate was calculated by the elongation of the rockbolt divided by the impact time. When the input energy is not sufficient to rupture the rockbolt, the middle sample test piece remains suspended on the deformed rockbolt. Vibration was evident in the rockbolt after the initial collision. After the stress wave in the rock has passed, the dynamic axial and shear strains gradually reduced in amplitude as the bolt continues to vibrate. For this situation, the rockbolt is capable of sustaining more input energy.

The failed rockbolts are shown in Fig. 14. The typical deformation of the rockbolt is described by two parameters, α and h as below, which were measured as the rockbolt was removed from the test unit after testing. These two parameters can describe the capacity of the shear resistance of rockbolt. Within this investigation, the 16-mm rockbolt is only bent, not sheared, as a result of insufficient energy input and exhibits ductility in that part

Table 4 Testing results

DST setup	Test number	Rebar failure types	Average dynamic load (kN)	Moving velocity (m s^{-1})	Shear displacement (mm)	Energy absorbed (J)
90°-Horizontal rebar	H-1	Rupture	77.5	3.8	25	1937
	H-2	Rupture	63.9	3.0	24	1533
	H-3	Rupture/bend	55.4	2.6	23	1274
	H-4	Bend	77.5	3.8	47.5	3681
45°-Inclined rebar	I-1	Rupture	63.9	3.0	21	2301
	I-2	Rupture/bend	55.4	2.6	23	1801
	I-3	Bend	55.4	2.6	20	1567
	I-4	Bend	77.5	3.8	25	2740

Fig. 13 Failed reinforced DST system after impact

of its strength curve. With the same input energy, the 45° inclined rockbolt has a smaller deformation than the horizontal rockbolt test. The inclined rockbolt system provides a greater shear resistance than the horizontal system. For

the 8-mm rockbolt, the shear displacement is over 24 mm causing the rockbolt to rupture in shear as seen in Fig. 14c.

The ruptured sections of rockbolt are shown in Fig. 15. The deformation of the rockbolt under impact loading may fail with little bending involved when it ruptures. This indicated that the rockbolt is subjected to localized shear force at the joint/plane intersection. Impact shear force is the dominant force to result in the failure of rockbolt, not the mobilized tensile force along the rockbolt. The fracture initiated close to two side blocks as shown in Fig. 15.

3.3 The Failure Types of Concrete Blocks Under Dynamic Load

Due to the brittle properties of the concrete, the design of the impact test should protect the concrete from damaging before the impact load fails the rockbolt element. One of the roles of confinement is to ensure the concrete sample remains intact at least during the initial period of contact. Therefore, the failure of concrete is only resulting from the vertical movement of rockbolt under dynamic load.

Fig. 14 Deformed rockbolt after impact

a. H-4

16 mm $\quad$ α=32°; h=47.5 mm;

b. I-4

16 mm $\quad$ α=13°; h=20 mm;

c. H-3

8 mm $\quad$ α=43°; h=25mm;

d. H-3

8 mm $\quad$ α=43°; h=24 mm;

Side Block 1 | Middle Block 2 | Middle Block 2 | Side Block 3
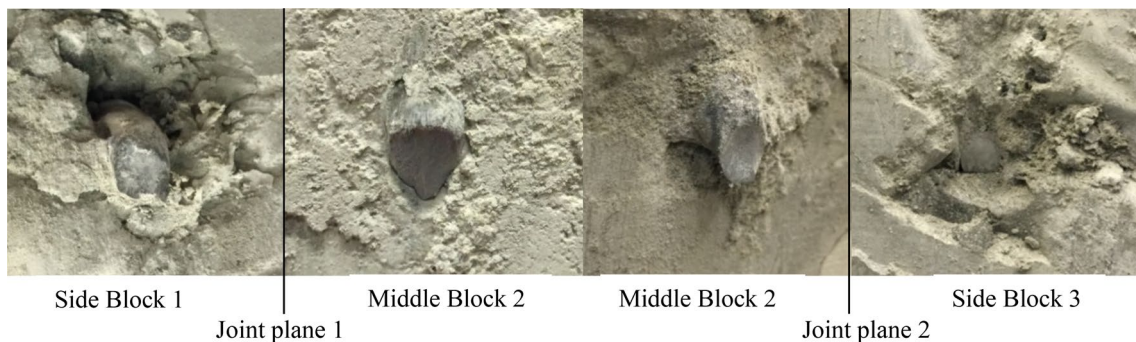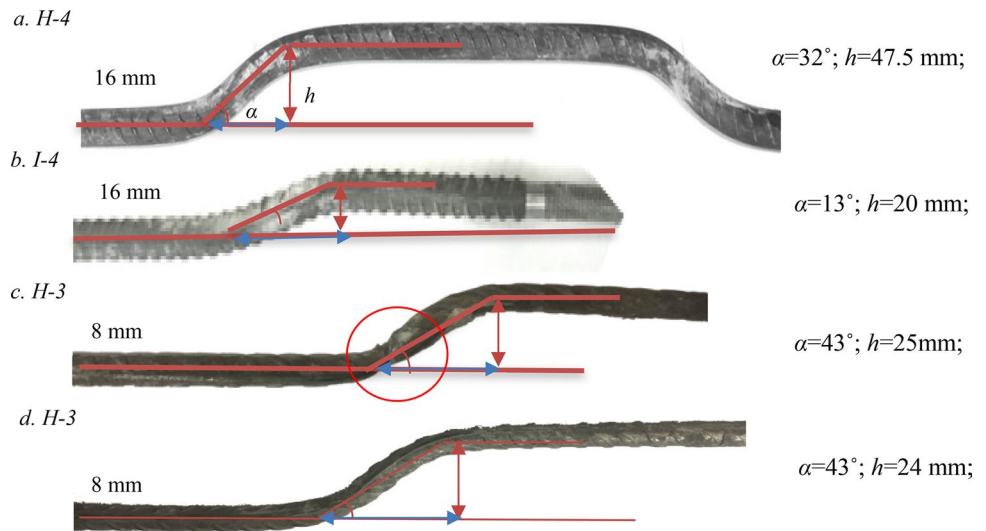Joint plane 1 | | Joint plane 2

Fig. 15 The ruptured section of 8-mm rockbolt

Figure 16 shows that concrete was crushed at the corner of the rockbolt and joint plane. This was a typical failure type of concrete surrounding the 8-mm rockbolt. Other than this localized failure, the concrete blocks had no large failure with the 8-mm rockbolt tests, as shown in Fig. 15.

The failure types of concrete embedded with 16-mm rockbolts are different to those with 8-mm rockbolts. The concrete samples cracked parallel to the direction of applied load and vertically along the plane of movement of the rockbolt, as shown in Fig. 17. When the applied dynamic force is not enough to rupture the rockbolt, the force transferred to the rockbolt results in bending of the rockbolt. The bending rockbolt transferred stress to the concrete block in an axial plane and caused a tensile failure of the concrete material.

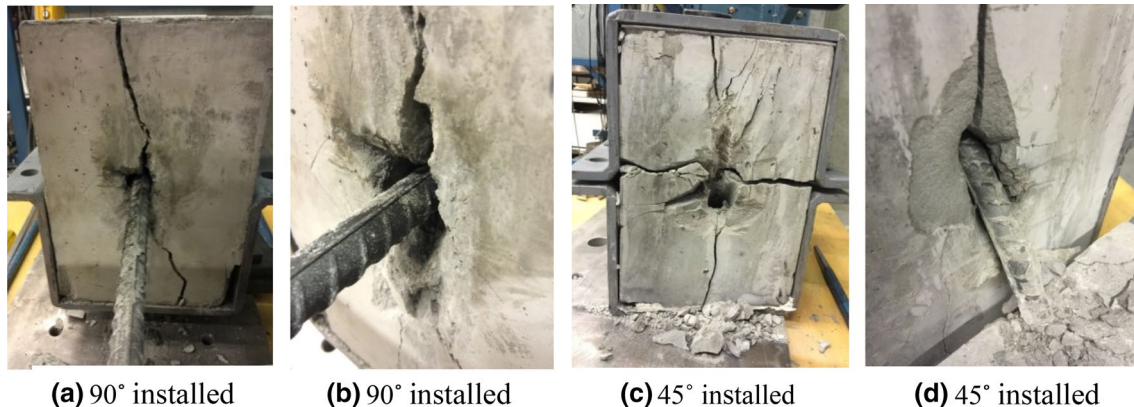**Fig. 16** Concrete was crushed around the joint intersection for inclined 8-mm rockbolt

3.4 The Energy Absorbed by DST System

The energy transferred from the drop weight to the DST system is calculated by the work done by the average dynamic load. Potvin et al. (2010) stated that the relationship between energy absorption and displacement from results of different bolts, tested on different rigs, using different protocols, are surprisingly consistent except for the friction bolt. The energy absorption for DST system is generally dissipated by bolt bending and elongation combined with gradual breaking of the grout/rock.

It can be seen that the energy absorbed by the inclined rockbolt is higher than the horizontal rockbolt (Fig. 18). For the 8-mm horizontal rockbolt, it was ruptured as the absorbed energy is close to 1219–1470 J, while the inclined rockbolt needed approximately 1807–2301 J to cause rupture. The testing facility is not sufficient to measure the maximum energy absorption for 16-mm rockbolt.

Figure 19 shows the relationship of total energy input (blue column) and the energy absorbed by rockbolt (red column). A rockbolt can only dissipate a limited amount of input energy. When the input energy is over the capacity of the rockbolt, the kinetic energy is dissipated by hitting the underlying platform of the test rig or causing damage to the concrete/grout.

4 Discussion

4.1 Equation of Motion for Dynamic System

The structure equilibrium under dynamic loading differs from static loading when considering the time-dependent loading conditions and inertial forces arising from mass acceleration. Figure 20 compared the force component when a single degree-of-freedom (SDOF) system subjected to static (a) and dynamic (b) loading.
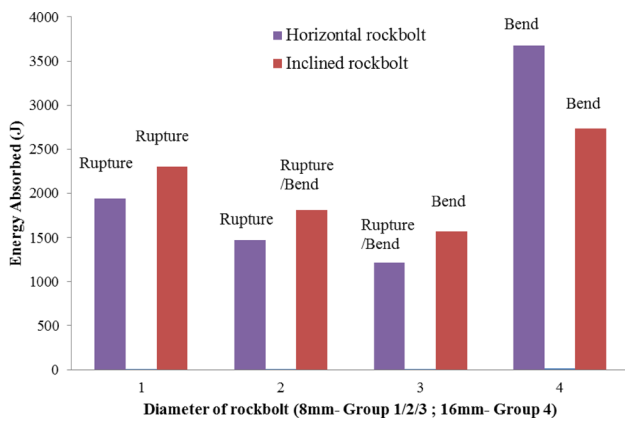

(a) 90° installed   **(b)** 90° installed   **(c)** 45° installed   **(d)** 45° installed

Fig. 17 Concrete samples cracked reinforced with 16-mm rockbolt

Fig. 18 Comparing the energy absorbed by horizontal and inclined rockbolt

When a system is subjected to static loading, the applied force (p) is resisted entirely by the spring force (f_s), as depicted in Fig. 20a. In contrast, in the dynamic system presented in Fig. 20b, the time-dependent force, $p(t)$, is resisted by a combination of the system spring force, $f_s(t)$, the viscous damping force, $f_D(t)$, and inertial force $f_I(t)$. The equation of motion of the dynamic system is presented as the following equation according to the Newton's second law of motion:

$$f_s(t) + f_D(t) + f_I(t) = p(t). \tag{4}$$

When two objects impact each other, the determination of impact force is crucial for the study of the motion after impact. Local indentation has a significant effect on the contact force history and must be accounted for in the analysis. During the impact of double shear system, the local indentation is small due to the deformation of the rockbolt and the buffer effect of carpet. During the loading phase of the impact, the contact force p is related to the indentation α according to the below equation (Abrate 2001):

$$p = k\alpha^{1.5}. \tag{5}$$

The contact stiffness is given as

$$k = \frac{4}{3}ER^{0.5}, \tag{6}$$

where the parameters R and E are defined in the following equations:

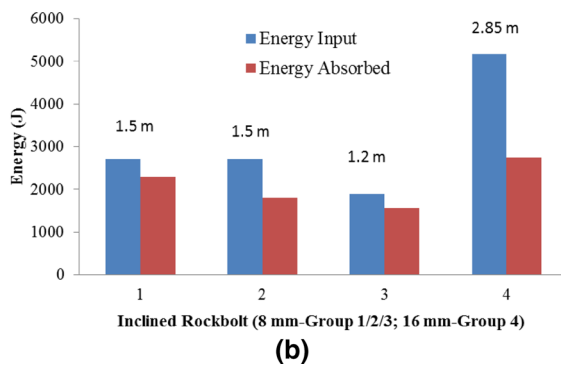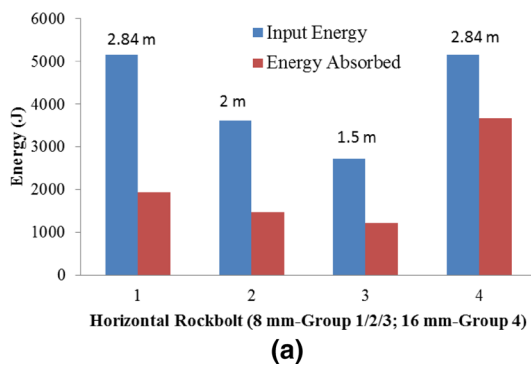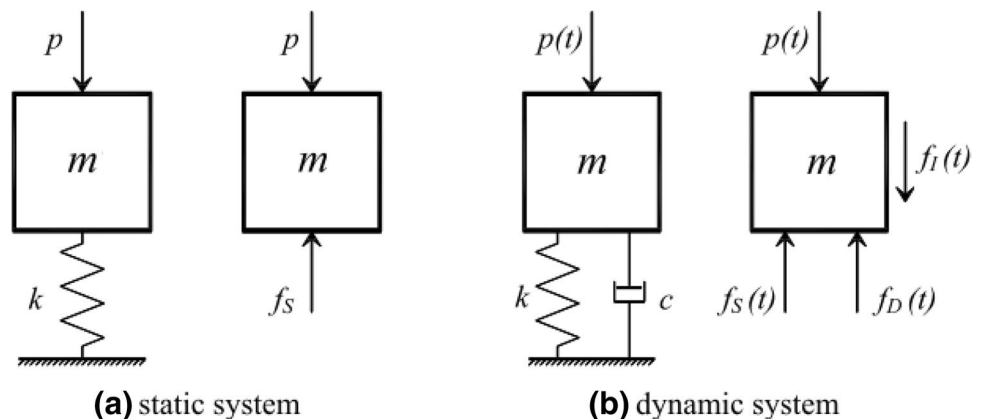$$\frac{1}{R} = \frac{1}{R_1} + \frac{1}{R_2}, \tag{7}$$

(a)

(b)

Fig. 19 Total energy input and energy absorbed by rockbolt. **a** Horizontal installation; **b** inclined installation. (Color figure online)

Fig. 20 SDOF force equilibrium (Saatci 2007)

(a) static system

(b) dynamic system

$$\frac{1}{E} = \frac{1 - v_1^2}{E_1} + \frac{1 - v_2^2}{E_2}, \tag{8}$$

where R_1 and R_2 are the radii of the curvature of the two bodies. The Young's modulus and Poisson's ratios of the two bodies are E_1, v_1 and E_2, v_2, respectively. Subscript 1 denotes properties of the impactor, while subscript 2 identifies properties of the target. In this double shear tests, the impact force calculation becomes difficult by Eq. (5) because of the carpet adoption between the impactor and target. It requires a caution use of carpet in the further dynamic testing in the case of impact force is critical.

4.2 Strain Rate Effects

The behaviours of structures subjected to high loading rates are not well understood, particularly in terms of the response at the material level. The experimental studies have demonstrated that the mechanical properties of the materials and structures are affected by the high rate of loading due to the structure's inability to respond quickly to the loading. The increase of strength properties under dynamic loading over static loading was commonly referred to as dynamic amplification factor (DAF) or dynamic increase factor (DIF). DIF is a dimensionless number which describes how many times the deflections or stresses should be multiplied to the deflections or stresses caused by the static loads when a dynamic load is applied to a structure (Argyris 1991).

In the case of plain concrete, both the concrete strength and stiffness are affected by the strain rate, and in the case of rockbolt, only strength parameter was amplified by the high strain rate. Several models were proposed for computing the DIF for concrete and steel rockbolt; Guner and Vecchio (2012) highlighted the large discrepancies amongst the

various relationships which have been proposed over the last 30 years (Fig. 21).

The rockbolt DIF model was developed by Malvar and Crawford (1998), and Malvar (1998) based upon a comprehensive review of experimental data. The authors stated that the DIF model is applicable for strain rates ($\dot{\varepsilon}$) between 10^{-4} and 225 s^{-1}, and is valid for the reinforcement element with static yield stresses ranging between approximately 290 and 710 MPa. The yield stress of rockbolt used in this study is within this range. Equation (9) indicates the dynamic increase factor for the yield stress of reinforcing bars, and Eq. (10) indicates the dynamic increase factor for ultimate stresses of reinforcing bars:

$$DIF_{fy} = \frac{\dot{\varepsilon}^{0.074 - 0.040\left(\frac{f_y}{414}\right)}}{10^{-4}}, \tag{9}$$

$$DIF_{fu} = \frac{\dot{\varepsilon}^{0.019 - 0.009\left(\frac{f_y}{414}\right)}}{10^{-4}}, \tag{10}$$

where f_y is the static yield stress of the bar in units of MPa. For the 8-mm rockbolts and the 16-mm rockbolts, the dynamic increase factors are listed as Table 5:

The main experimental technique for the dynamic characterisation of metal material is the Split Hopkinson Pressure Bar testing system (Staker 1985) within the range of 102–104 s^{-1}. It should be stated that these high-strain-rate experiments are accompanied by a noticeable temperature rise in the specimen, which causes thermal softening of the overall mechanical response of the specimen. The Johnson–Cook (1983) model was developed and gave a linear increase of the true stress with the logarithm of the strain rates as Eq. (11), which is a product of three factors: strain hardening, strain-rate hardening, and a thermal softening
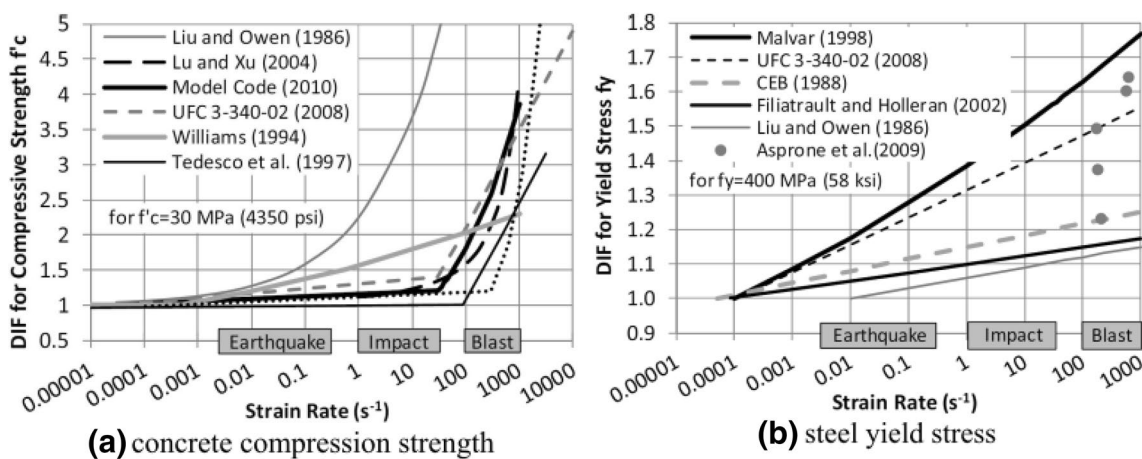

Fig. 21 Comparison of proposed dynamic increase factor (Guner and Vecchio 2012)

Table 5 The dynamic increase factor with 1 s^{-1} strain rate

Dynamic increase factor	8 mm	16 mm
DIF$_{fy}$	1.33	1.19
DIF$_{fu}$	1.06	1.04

term (Qin et al. 2013). Within this study, thermal softening term was omitted:

$$\sigma = \left(A + B\varepsilon_p^n\right)\left(1 + CIn\frac{\dot{\varepsilon}}{\dot{\varepsilon}_0}\right)\left[1 - \left(\frac{T - T_{room}}{T_{melt} - T_{room}}\right)^m\right], \tag{11}$$

where ε_p is the true strain, $\dot{\varepsilon}$ is the strain rate, $\dot{\varepsilon}_0$ is the reference value of the strain rate, T is the temperature, T_{room} is room temperature, and T_{melt} is melting temperature. The Johnson–Cook plasticity model is suitable for high-strain-rate deformation of many materials. However, the determination of the coefficients A, B, n, C needs complicated experimental tests. This double shear test is not related to the determination of these Johnson–Cook parameters. Despite the difficulty of Johnson–Cook parameter determination, the yield strength or ultimate strength of rockbolt will increase as the strain rate increases.

Many experimental studies have presented the results of strain-rate-dependent characteristics, such as Fig. 22 described by Kim et al. (2013). The increase of strength and elongation with increasing strain rate can be seen from Fig. 22. It can also be concluded that the low velocity impact (3 m s^{-1}) and the low strain rate (1 s^{-1}) have only minor effects on the dynamic properties of the steel bar. Therefore, we assume the dynamic strength properties of the rockbolt will not be significantly changed due to impact loading applied.

4.3 Comparison of DST Under Static and Dynamic Loading Conditions

The double shear tests reinforced with rebar were performed under static and dynamic loading conditions. A comparison was conducted in terms of shear load, rockbolt deformation and energy absorbed to reveal the shear mechanism of the rockbolt under different strain rates.

The peak shear loads occurred during the static tests averaged at 51.5 kN for horizontally installed rockbolts and 65.5 kN for 45° installed rockbolts, which is 1.78 times and 2.26 times the tensile strength of the rockbolt, respectively, as listed in Table 6. It is observed that this shear load subjected to rockbolt also causes elongation of the rockbolt in the axial direction. The higher peak shear load can be attributed to a higher initial stiffness of DST system. However, under dynamic loading conditions, this greater stiffness
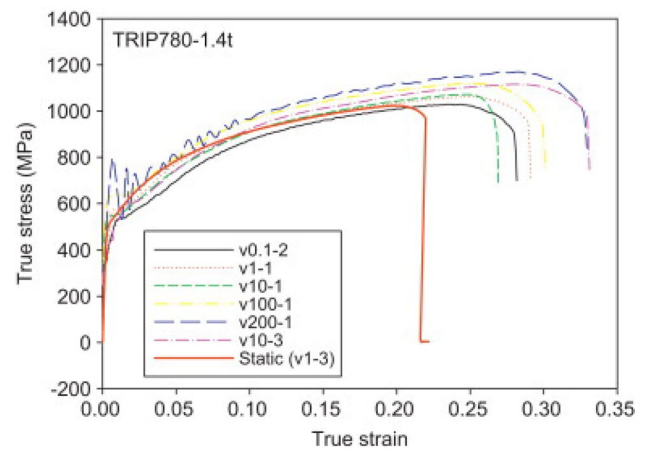

Fig. 22 True stress–strain curves of steel under various strain rates (Kim et al. 2013)

becomes a weakness, which allows brittle failure of the rebar to occur, rather than the shear-tensile failures observed in the static tests. The averaged shear load for 8-mm rockbolt is about 39 kN under dynamic loading conditions. Therefore, although the averaged dynamic load is smaller than the static peak shear load, the rockbolt can resist more than 1.34 times of ultimate tensile load of rockbolt under dynamic condition.

Rockbolt slippage was observed in almost all double shear tests performed, which refers to the distance of rockbolt debonded from the grout. Similar failures of rockbolts were observed in both static and dynamic shear tests, but it has been observed that a smaller slippage range occurred under the dynamic conditions. The 8-mm rockbolt suffered an immediate failure due to bending, approximately 20 mm away from the shear plane on the side of the stationary blocks under dynamic loading conditions, as shown in Fig. 23a, and 25 mm away from the shear plane under the static loading conditions. A ductile failure occurred under static loading conditions, because the range of slippage is bigger compared to the dynamic tests for 16-mm rockbolt. The slippage occurs away from the two shear planes 45 mm and 35 mm, respectively, as shown in Fig. 23b. Generally, the rockbolt bends on both sides of shear plane under strain rate of 0.001 s^{-1}, while the rockbolt is inclined to bend at

Table 6 Comparison of the shear load subjected to rockbolt for static and dynamic DST (half of double shear testing results)

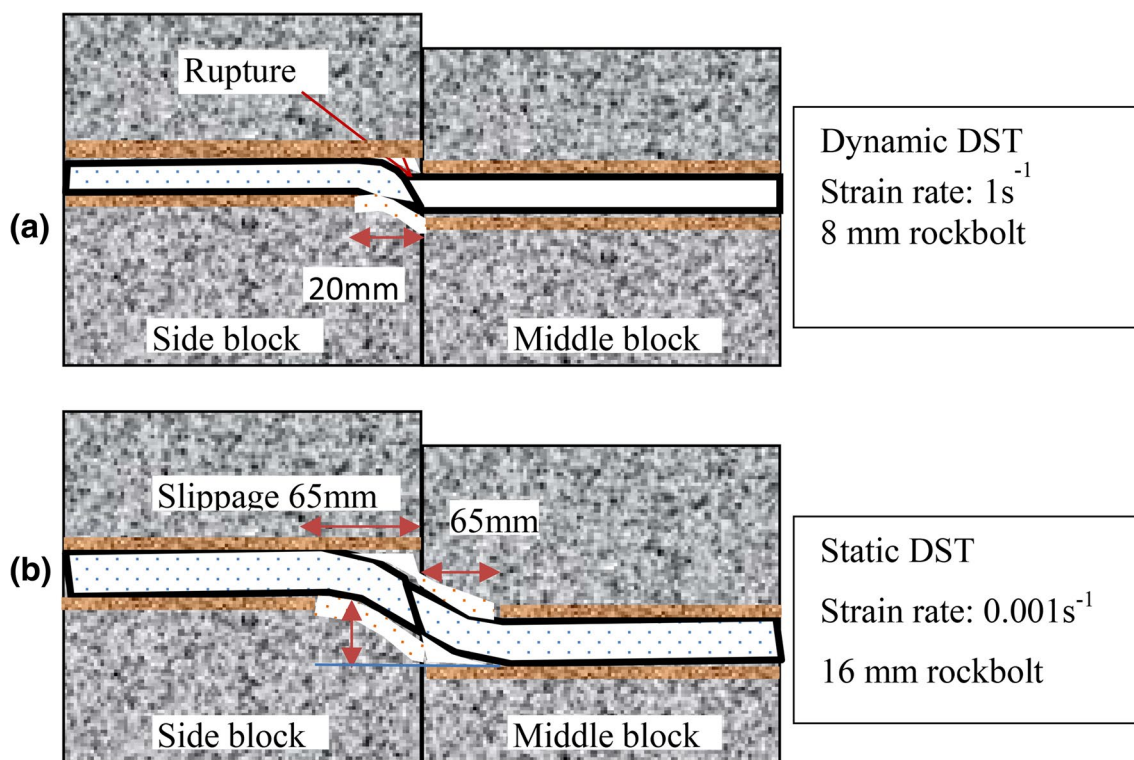| Rockbolt diameters, installation angle, and rockbolt failure types	Peak shear load Static (kN)	Averaged dynamic load Dynamic (kN)
8 mm		
90° ruptured	51.5	39
45° bend at 25 mm	67.5	> 39

Fig. 23 Illustration of observed failure of rockbolt in static and dynamic double shear

only side block under strain rate of 1 s⁻¹. The range of slippage of rockbolt was averaged and is listed in Table 7.

Table 8 shows the energy absorbed by the rockbolts when subjected to static and dynamic loading conditions. Under the same deformation of an 8-mm rockbolt, the energy absorbed under dynamic loading conditions is less than under the static loading conditions. This is because of the small range of rockbolt slippage and small vertical displacement mobilized along the rockbolt as described in the above section. Another reason is that the ultimate strain and the slope of the strain-hardening curve decrease with increasing strain rate (Roberts 1999).

In conclusion, the difference of shear performance of rockbolts under static and dynamic loading is summarized as follows:

- Rockbolts can resist higher shear load when subjected to dynamic load than static load conditions.
- Rockbolts have a smaller range of slippage when subjected to dynamic load than static load conditions.
- Rockbolts absorb less energy when subjected to dynamic load than static load conditions.

Table 7 Comparison of static and dynamic rockbolt slippage range

Rockbolt diameters and installation angle	Average rockbolt slippage range at one side of shear plane		Average vertical displacement	
	Static (mm)	Dynamic (mm)	Static (mm)	Dynamic (mm)
8 mm ruptured				
90°	25–30	20–25	25	24
45°	25–35	25–30	16	15
16 mm bent				
90°	90–120	70–80	76	47
45°	80–90	70–80	35	15

Vertical displacement is the direction perpendicular to the direction of the rockbolt

**Table 8** Comparison of the energy absorbed by static and dynamic DST

Rockbolt diameters, installation angle, and rockbolt failure types	Energy absorbed by rockbolt	
	Static (J)	Dynamic (J)
8 mm		
90° ruptured	2102	1219–1470
45° bend at 25 mm	2925	1807–2301

4.4 Recommendations for the Optimisation of Drop Test

When conducting the drop tests, following actions should be avoided during the tests to ensure the accuracy of the measurement, including

1. *Imbalanced loading* When impact load is applied to the middle concrete block, the horizontal load occurred due to the bending of the rockbolt, which leads to the side blocks becoming inclined, as shown in Fig. 24. Another action resulting in the imbalanced loading is the position of steel plate at the bottom of sample, it should be put near the joint plane and develops the support role. In one test, the sample was set up as shown in Fig. 24, as a result the vibration of the sample was more intense. The intense vibration of the sample increases the frictional force between the two blocks. Therefore, this imbalanced loading should be avoided during the tests, and the sample should be maintained as stable as possible.

2. *Inertial force* The force of inertia is the property common to all bodies that remain in their state, either at rest or in motion, unless some external cause is introduced to make them alter this state. At the moment of impact, the impact load would include the inertial response of the specimen, the support reaction would not. It is one of the reasons why the peak shear dynamic force is not obtained from this impact testing. One potential method of eliminating inertial forces in a drop tests is by measuring the support reaction by installing the load cell under both sides of concrete blocks.

At first, the capacity of this rig was not sufficient to achieve the level of dynamic shear capacity required to shear or fail a 16-mm rebar and an inclined installed rebar. A heavier drop weight or a higher drop height was required to get the dynamic shear capacity of these rockbolts. The encapsulation length of 16 mm in concrete is insufficient to stop bolt being pull out during dynamic shearing of the double shear assembly, leading to the bolt being debonded with the pulled out section undergoing bending. Also the cracking of the concrete would compound the situation.
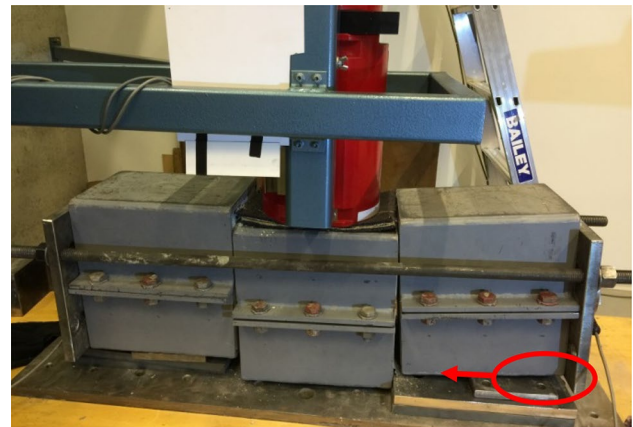
Fig. 24 The imbalanced position

Second, acceleration data recorded in these tests were the impact acceleration measurement, which cannot be used to calculate the dynamic force applied on the rockbolt. Therefore, the dynamic load cell is preferably used as a direct dynamic load measurement. It was recommended that further tests should be performed considering the above two suggestions and to circumvent the above two issues.

5 Conclusion

An extensive study of the dynamic shear response of a rockbolt subjected to impact load by a falling mass was undertaken. The influencing parameters, including installation angle, rockbolt diameter and input energy, were examined in laboratory tests. A comparison between static and dynamic responses of rockbolts is very important as the dynamic behaviour of the rockbolt reflects the performance under rockburst conditions.

When sufficient energy is input into the DST system, the deformation of the rockbolt is dominated by localized shear force. The transient force can rupture the rockbolt with little bending and without an obvious tensile elongation. A lower drop height generated a combination of shear and tensile force around the joint plane. This situation is like the quasi-static loading condition. It can be concluded that rockbolt shear deformation is dominated by axial elongation and shear resistance. Therefore, the dynamic shear performance of a rockbolt is strain rate dependent.

This designed DST is incapable of explaining the shear strength of a rockbolt under dynamic loading conditions. Therefore, this study does not discuss the inherent properties of rockbolt material under impact loading. The following three aspects were compared for the static and dynamic DST: peak/average shear load, rockbolt deformation and energy absorption capacity.

It was found that the averaged dynamic shear load is less than peak static shear load for 8-mm rockbolt whether horizontally installed or installed at an angle. However, the dynamic peak load is possibly higher than the static peak load because the dynamic peak shear load is far more than averaged force. Although the load bearing capacity is one of the significant parameters to evaluate the performance of a rockbolt system, we cannot conclude that the rebar alone is suitable to be used in the rockburst conditions. In general, a rockburst occurrence results in a larger deformation of the tunnel surface. In other words, the rebar should be equipped with the ability to resist large deformation. However, rebar shows an inadequate ability to resist larger shear deformation.

It was observed that the rockbolt failed within 10–12 ms under impact loading. The 8-mm rockbolt was ruptured with a 20-mm slippage range, which is smaller compared to the 25-mm slippage range under static loading. Similarly, for the 16-mm rockbolt, approximately 70–80 mm of slippage occurred at the both sides of shear plane under dynamic loading, while 90–120 mm of slippage occurred under static loading. It is worth noting that there is no significant difference in the ultimate shear displacement of a 8-mm rockbolt, which is also demonstrated by Roberts (1999). A large variation was displayed in the 16-mm rockbolt results because the rockbolt was not ruptured using the current experimental system.

The installation angle of a rockbolt with a joint does influence the shear resistance of the rockbolt. This study concluded that the 45° inclined rockbolt has less deformation compared to the horizontally installed rockbolt when same energy is input into the DST system irrespective of static or dynamic loading conditions.

Although the shear demand on the rockbolt system has not been quantified in this investigation, the above analysis will allow the support design engineer to implement the most appropriate rockbolt reinforcement system where shear deformations are anticipated. In conclusion, the shear capacity of a rockbolt under 1 s^{-1} strain rate can be determined by the energy absorbed and average dynamic load, and it provides an insight for the support design under seismicity condition.

Compliance with ethical standards

Conflict of interest All authors declare that they have no conflict of interest.

References

Abrate S (2001) Modeling of impacts on composite structures. Compos Struct 51:129–138. https://doi.org/10.1016/S0263-8223(00)00138-0

Argyris JH (1991) Dynamics of structures. North-Holland, New York

Aziz N, Pratt D, Williams R (2003) Double shear testing of bolts. In: Aziz N (ed) Coal operators' conference, Wollongong, Australia, pp 154–161

Bischoff PH, Perry SH (1991) Compressive behaviour of concrete at high strain rates. Mater Struct 24:425–450. https://doi.org/10.1007/BF02472016

Chung HW (1978) Shear strength of concrete joints under dynamic loads. Concrete 12:27–29

Grasselli G (2005) 3D behaviour of bolted rock joints: experimental and numerical study International. J Rock Mech Mining Sci 42:13–24. https://doi.org/10.1016/j.ijrmms.2004.06.003

Guner S, Vecchio FJ (2012) Simplified method for monlinear dynamic analysis of shear-critical frames. ACI Struct J 109:10

Hadjigeorgiou J, Potvin Y (2011) A critical assessment of dynamic rock reinforcement and support testing facilities. Rock Mech Rock Eng 44:565–578. https://doi.org/10.1007/s00603-011-0155-4

Haile AT (1999a) A mechanistic evaluation and design of tunnel support systems for deep level South African mines. PhD thesis (unpublished), University of Natal

Haile AT (1999b) Observation of the dynamic support performance of South African tunnel support systems. In: Villaescusa E, Windsor CR, Thompson A (eds) Rock support and reinforcement practice in mining, Kalgoorlie, Australia, pp 335–341

Jalalifar H (2006) A new approach in determining the load transfer mechanism in fully grouted bolts. PhD thesis (unpublished), University Of Wollongong

Johnson GR, Cook WH (1983) A constitutive model and data for metals subjected to large strains, high strain rates and high. In: The 7th international symposium on ballistics, pp 541–547

Kim J-H, Kim D, Han HN, Barlat F, Lee M-G (2013) Strain rate dependent tensile behavior of advanced high strength steels: experiment and constitutive modeling. Mater Sci Eng A 559:222–231. https://doi.org/10.1016/j.msea.2012.08.087

Kong S, Remennikov A, Uy B (2013) An experimental investigation of the performance of non-composite steel–concrete–steel protective panels under large impact loading. Adv Struct Eng Int J 16:1163–1174

Li C (2011) Rock support for underground excavations subjected to dynamic loads and failure. Adv Rock Dyn Appl. https://doi.org/10.1201/b11077-19

Li L, Hagan P, Saydam S (2014) Tensile stress mobilization along a rockbolt under shear load. In: Cai M (ed) International young scholars' symposium on rock mechanics, Xi'an, China

Li L, Hagan P, Saydam S, Hebblewhite B (2016) Shear resistance contribution of support systems in double shear test. Tunnel Undergr Space Technol 56:8

Malvar LJ (1998) Review of static and dynamic properties of steel reinforcing bars. Mater J 95:609–616. https://doi.org/10.14359/403

Malvar LJ, Crawford JE Dynamic increase factors for steel reinforcing bars. In: Twenty-Eighth DoD Explosives Safety Seminar, Orlando, United State, 1998. Naval Facilities Engineering Service Center

Potvin Y, Wesseloo J, Heal D (2010) An interpretation of ground support capacity submitted to dynamic loading. Trans Inst Mining Metall Sect A Mining Technol 4:233–245

Qin J, Chen R, Wen X, Lin Y, Liang M, Lu F (2013) Mechanical behaviour of dual-phase high-strength steel under high strain rate tensile loading. Mater Sci Eng A 586:62–70. https://doi.org/10.1016/j.msea.2013.07.091

Roberts D (1999) Dynamic double shear test. PhD thesis (unpublished), University of KwaZulu-Natal

Saatci S (2007) Behaviour and modeling of reinforced concrete structures subjected to impact loads. PhD thesis (unpublished), University of Toronto

Stacey TR Support of excavations subjected to dynamic loading. In: Qian Q, Zhou Y (eds) 12th ISRM International Congress on Rock

Mechanics, Beijing, China, 2011. International Society for Rock Mechanics, ISRM

Staker MR (1985) Mechanical testing; chapter: introduction to high strain rate testing, 9th edn. ASM International, New York

Tannant DD, Brummer RK, Yi X (1995) Rockbolt behaviour under dynamic loading: field tests and modelling. Int J Rock Mech Mining Sci Geomech Abstracts 32:537–550. https://doi.org/10.1016/0148-9062(95)00024-B

Zembaty Z (2011) How to model rockburst seismic loads for civil engineering purposes? Bull Earthq Eng 9:1403–1416. https://doi.org/10.1007/s10518-011-9269-z